



Title	Phase transitions of dense systems of charged "dust" grains in plasmas
Author(s)	Farouki, R. T.; Hamaguchi, S.
Citation	Applied Physics Letters. 1992, 61(25), p. 2973-2975
Version Type	VoR
URL	<a href="https://hdl.handle.net/11094/78512">https://hdl.handle.net/11094/78512</a>
rights	This article may be downloaded for personal use only. Any other use requires prior permission of the author and AIP Publishing. This article appeared in Appl. Phys. Lett. 61, 2973 (1992) and may be found at <a href="https://doi.org/10.1063/1.108035">https://doi.org/10.1063/1.108035</a> .
Note	

*The University of Osaka Institutional Knowledge Archive : OUKA*

<https://ir.library.osaka-u.ac.jp/>

The University of Osaka

# Phase transitions of dense systems of charged “dust” grains in plasmas

Cite as: Appl. Phys. Lett. **61**, 2973 (1992); <https://doi.org/10.1063/1.108035>

Submitted: 27 July 1992 . Accepted: 14 October 1992 . Published Online: 05 August 1998

R. T. Farouki, and S. Hamaguchi



View Online



Export Citation

## ARTICLES YOU MAY BE INTERESTED IN

[Phase diagram of Yukawa systems near the one-component-plasma limit revisited](#)

The Journal of Chemical Physics **105**, 7641 (1996); <https://doi.org/10.1063/1.472802>

[Coulomb solid of small particles in plasmas](#)

The Physics of Fluids **29**, 1764 (1986); <https://doi.org/10.1063/1.865653>

[Thermodynamics of strongly-coupled Yukawa systems near the one-component-plasma limit. II. Molecular dynamics simulations](#)

The Journal of Chemical Physics **101**, 9885 (1994); <https://doi.org/10.1063/1.467955>



## Your Qubits. Measured.

Meet the next generation of quantum analyzers

- Readout for up to 64 qubits
- Operation at up to 8.5 GHz, mixer-calibration-free
- Signal optimization with minimal latency

Find out more



# Phase transitions of dense systems of charged "dust" grains in plasmas

R. T. Farouki and S. Hamaguchi

IBM Thomas J. Watson Research Center, P. O. Box 218, Yorktown Heights, New York 10598

(Received 27 July 1992; accepted for publication 14 October 1992)

The behavior of "dust" grains (particulates) in microelectronics process plasmas has been studied using  $N$ -body simulations. Grains are assumed to be negatively charged and interact through a screened Coulomb potential  $\Phi(r)$ . The dimensionless parameters  $\kappa = a/\lambda$  and  $\Gamma = \Phi(a)/k_B T$  characterize the thermodynamics of the particulate system, where  $\lambda$  is the ion Debye length,  $a = (3/4\pi n_D)^{1/3}$  is the mean intergrain distance, and  $n_D$  and  $T$  are the dust density and temperature. The simulations exhibit a transition between "fluid" and "solid" phases at a critical value  $\Gamma_c$  that depends on  $\kappa$  and weakly on the system history (i.e., whether it "melts" from an ordered state or "freezes" from a random one).

Particulate or "dust" contamination has attracted much interest among the microelectronics process plasma community.<sup>1-4</sup> The particulates are observed to be negatively charged and tend to accumulate near the plasma-sheath boundary. Since the deposition of particulates on a semiconductor wafer during plasma processing can severely impact the yield of defect-free chips, an understanding of the thermodynamical and transport properties of particulate systems immersed in plasmas is of great practical importance.

This letter presents preliminary results of  $N$ -body simulations addressing this problem. As noted by Ikezi,<sup>5</sup> under representative discharge conditions the interparticle potential energy can greatly exceed the kinetic energy. By analogy with the classical one-component plasma<sup>6,7</sup> one expects the possibility of a fluid-solid phase transition in particulate systems under suitable conditions (another physical analog is the formation of lattices by colloidal suspensions<sup>8,9</sup>). We have observed such transitions by directly integrating the equations of motion of interacting charged grains.

The potential distribution around grains in a plasma has been studied in detail, especially in the astrophysical context.<sup>10</sup> It is generally understood that grains are negatively charged and surrounded by sheaths characterized by a Debye length  $\lambda = (1/\lambda_i + 1/\lambda_e)^{-1}$ , where  $\lambda_i$  and  $\lambda_e$  are the ion and electron Debye lengths. Since  $\lambda_e \gg \lambda_i$  under conditions that concern us, we have  $\lambda \simeq \lambda_i$ . The detailed structure of these sheaths depends on parameters such as the plasma collisionality and the ratio  $\kappa = a/\lambda$  of the intergrain distance  $a = (3/4\pi n_D)^{1/3}$ , where  $n_D$  is the dust density, to the Debye length. To facilitate the simulations, we adopt the simple screened Coulomb form

$$\Phi(r) = \frac{Q^2}{4\pi\epsilon_0 r} \exp(-r/\lambda)$$

for the interaction potential between particulates of charge  $Q$  at distance  $r$  apart, which is known to be a good approximation when  $\kappa$  is not small.<sup>10</sup>

In addition to  $\kappa$ , the thermodynamics of the particulate system depends on only one additional dimensionless parameter: the ratio  $\Gamma = \Phi(a)/k_B T$  of typical grain potential and kinetic energies ( $T$  is the dust temperature). For typ-

ical process plasma conditions—e.g., ion density  $n_i = 10^{10} \text{ cm}^{-3}$  and temperature  $T_i = 0.5 \text{ eV} \ll T_e$ , and dust density  $n_D = 5 \times 10^6 \text{ cm}^{-3}$ , temperature  $T = 0.1 \text{ eV}$ , and charge  $Q = Z_D e = 10^3 e$ —we have  $\kappa \approx 0.7$  and  $\Gamma \approx 200$ . Here  $T_e$  denotes the electron temperature, and the free electron density  $n_e$  is determined by charge balance:  $n_e = n_i - Z_D n_D = 5 \times 10^9 \text{ cm}^{-3}$  in this case. For sufficiently high  $n_D$ , the free electrons are entirely depleted and we have  $Z_D = n_i/n_D$ .

In the simulations we take as units of mass, length, and time, the grain mass  $m_D$ , the intergrain spacing  $a$ , and  $\sqrt{3}\omega_D^{-1}$  where  $\omega_D = \sqrt{Q^2 n_D / \epsilon_0 m_D}$  is the dust plasma frequency. The equations of motion are then

$$\frac{d^2 \xi_k}{dt^2} = \sum_{j \neq k}^N \exp(-\kappa \xi_{kj}) \frac{1 + \kappa \xi_{kj}}{\xi_{kj}^3} (\xi_k - \xi_j)$$

for  $k = 1, \dots, N$  where  $\xi_{kj} = |\xi_k - \xi_j|$ . We integrate them using a predictor-corrector scheme, in which the variation of the force on a particle over each step is extrapolated from a quadratic fitting polynomial that interpolates its value at three preceding instances. An *a posteriori* cubic "correction" term enhances the accuracy of the position and velocity increments. Forces are obtained by explicit pairwise summation over *all* particles. Since the phase transitions are characterized by minuscule fractional energy changes ( $< 1\%$ ), we make no concession to efficiency at the expense of integration accuracy. The integration proceeds on an asynchronous timefront, with individually adjusted steps to ensure uniformly accurate trajectories under widely varying conditions. The particles are periodically synchronized to sample system properties before restarting. Fractional energy errors between successive starts were confined to the range  $10^{-5}$ – $10^{-6}$ .

The particles are initially placed in a cubical simulation volume  $V$  of dimension  $L = (4\pi N/3)^{1/3} a$ , either at random or on a simple cubic lattice, and are given Maxwellian velocities corresponding to the target  $\Gamma$  value ( $N$  must be chosen such that  $L/\lambda$  is substantially greater than unity). In order to emulate an infinite system, we employ periodic boundary conditions: the basic simulation volume  $V$  is surrounded by neighboring copies  $V'$  of itself, and each particle  $k$  interacts with particle  $j$  in  $V$  or with an image of  $j$  in one of the copies  $V'$  according to whichever is

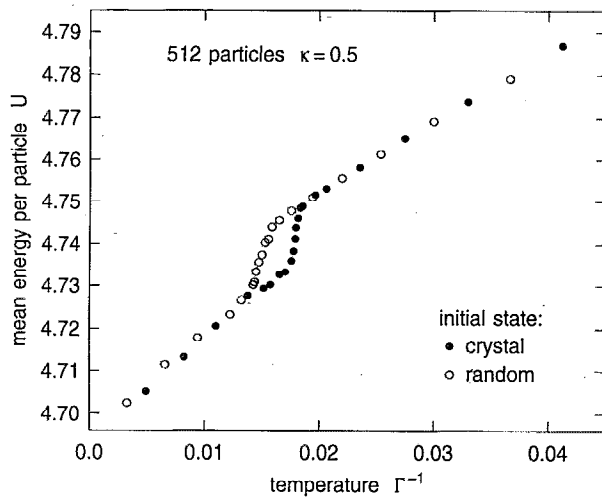


FIG. 1. Variation of the steady-state internal (kinetic+potential) energy per particle  $U$  with temperature  $\Gamma^{-1}$  for  $\kappa=0.5$  with  $N=512$ . Two sets of runs were performed, commencing with particles distributed randomly and on a cubic ( $8 \times 8 \times 8$ ) lattice. Note the dependence of the critical value  $\Gamma_c$  on the initial state: starting from random configurations the particulate system forms a "supercooled liquid" before freezing, whereas it becomes a "superheated crystal" before melting when started from ordered configurations.

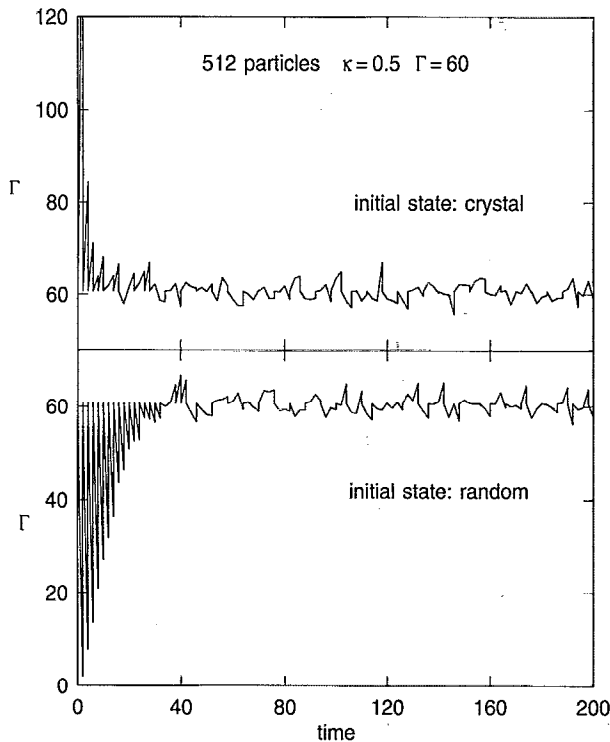


FIG. 2. The time dependence of  $\Gamma$  in typical runs, showing the effect of cooling/heating to achieve a prescribed mean temperature. Note the rapid development of dynamical equilibrium from both ordered and random initial states. The data of Fig. 1 are averages between  $\tau=100$  and 200 (temperature fluctuations during this interval are consistent with the constraints of the cooling/heating mechanism).

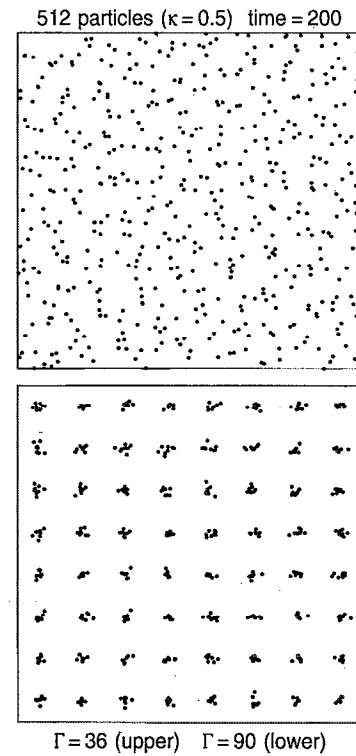


FIG. 3. Final "liquid" and "solid" states of the particulate system, at  $\Gamma=36$  and  $90$  ( $\Gamma^{-1}=0.028$  and  $0.011$ ), respectively. The plots show  $(x,y)$  projections of the particle positions at  $\tau=200$ , starting from a crystalline initial state in each case.

nearest. The system has positive total energy, and is assumed to be maintained at constant density  $n_D=N/V$  by the action of a "trap" with near-uniform interior potential.<sup>4</sup>

Nominally, time averages of unperturbed  $N$ -body simulations correspond to microcanonical ensemble averages for systems of fixed total energy  $E$ . To model a canonical ensemble of fixed  $\Gamma$  (temperature) we introduce periodic cooling/heating of the system by renormalizing particle velocities<sup>11</sup> to the target  $\Gamma$  value. With a free exchange of potential and kinetic energies during the integration periods, this scheme yields systems in dynamical equilibrium at a given mean temperature whose properties can be time averaged.

Using 216, 512, and 1000 particles, sequences of runs with  $\kappa=0.5$  and various  $\Gamma$  values were performed, starting from both random and crystalline initial states. Figure 1 shows data for the case  $N=512$ . Each run was evolved for 200 time units, with synchronization at 2-unit intervals for sampling and temperature adjustments. The internal energy data<sup>12</sup> was averaged over  $100 < \tau \leq 200$ , by which time the system had fully settled (as can be seen from representative examples for the evolution of  $\Gamma$  in Fig. 2). The phase transition is characterized by a sudden change in the internal energy per particle at the critical temperature  $\Gamma_c^{-1}$ , whose value is evidently dependent on "memory" of the initial state. Analogous results have been observed in the freezing/melting of ionic salts.<sup>13,14</sup>

Lest there be any doubt about the interpretation of the

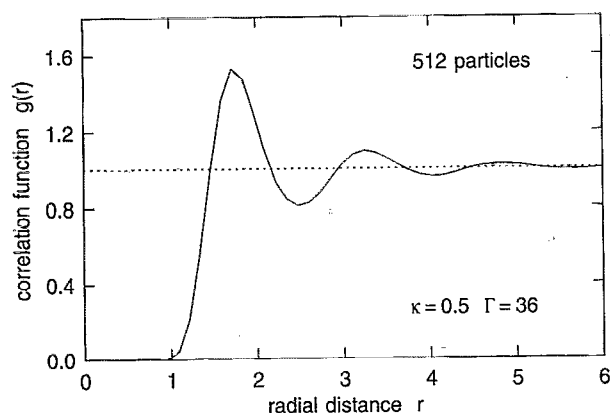


FIG. 4. The radial pair correlation function  $g(r)$ —which represents the probability of finding a particle at distance  $r$  from a given particle—observed in a typical run at a temperature above the phase transition. The short-range order evident in  $g(r)$  is characteristic of the “liquid” state.

jumps in Fig. 1, we show in Fig. 3 pictorial representations of the final particle distributions for  $\Gamma$  values below and above  $\Gamma_c$ . Note also that for  $1 \leq \Gamma < \Gamma_c$ , it is appropriate to characterize the particulate system as a “liquid” rather than a “gas.” Figure 4 shows the pair correlation function  $g(r)$  when  $\Gamma = 36$ , in which the distinctive short-range order of a liquid system is apparent—the first peak coincides with the nearest-neighbor distance of an fcc lattice.

Preliminary experiments show that  $\Gamma_c$  is sensitive to the interaction range  $\kappa$  (when  $\kappa \gg 1$ , the ability of the particulate system to condense at all is severely compromised). Another important concern is the  $N$  dependence of  $\Gamma_c$ . Because of Debye screening, the potential energy per particle of a finite simple cubic lattice—subject to periodic boundary conditions—converges rapidly with  $N$  to its asymptotic Madelung value. With  $N=216$ , 512, and 1000, for example, the potential energy is 74.9%, 87.9%, and 94.4% of the Madelung value (when  $\kappa=0.5$ ); corresponding values of  $L/\lambda$  are 4.84, 6.45, and 8.06. Nevertheless, the critical temperature  $\Gamma_c^{-1}$  was observed to decrease systematically with system size over the limited range we have explored:  $\Gamma_c=31$ –33 for  $N=216$ , 58–67 for  $N=512$  (see Fig. 1), and  $\Gamma_c \gtrsim 100$  for  $N=1000$ .

Several problems arise in attempting to extrapolate our results to identify the critical value  $\Gamma_c$  that is appropriate to the limit  $N \rightarrow \infty$ . Apart from the computational expense, in large systems the dynamics of lattice defects (and the constraints imposed on them by periodic boundary conditions) play an important role. Also, condensation into a simple cubic lattice is predicated on choosing  $N=\nu^3$  for integer  $\nu$ , provided  $N$  is not too large. For large systems,

however, imperfect bcc or fcc lattices may be favored (perfect forms require  $N=2\nu^3$  and  $4\nu^3$ , respectively). Such effects were already noticeable in the runs starting from random initial states with  $N=1000$ . We quoted only a *lower bound* on  $\Gamma_c$  for this sequence because of a strong tendency to form a “supercooled” liquid at  $\Gamma > 100$  when starting from a random state; those cases that did crystallize appeared to be unstable with respect to stochastic fluctuations and of defective bcc form (note that  $2 \times 8^3 = 1024$ ). These considerations are currently under more thorough investigation.

Thermodynamically, phase transitions in systems of prescribed density and temperature are usually characterized by the behavior of derivatives of the Helmholtz free energy  $F=U-TS$  per particle (where  $S$  is the entropy per particle). The transitions we have observed appear to be first order; the particulate-system thermodynamics will be addressed in a future paper.

*Note added in proof:* It has come to our attention that other authors—e.g., M. O. Robbins, K. Kremer, and G. S. Grest, *J. Chem. Phys.* **88**, 3286 (1988); E. J. Meijer and D. Frenkel, *J. Chem. Phys.* **94**, 2269 (1991)—have recently studied “Yukawa systems” (i.e., particles interacting through a screened Coulomb potential) using molecular dynamics and Monte Carlo techniques. Although motivated primarily by the physical context of colloidal suspensions, their results are applicable to the plasma/dust system described herein.

<sup>1</sup>K. G. Spears, T. J. Robinson, and R. M. Roth, *IEEE Trans. Plasma Sci.* **14**, 179 (1986).

<sup>2</sup>G. S. Selwyn, J. Singh, and R. S. Bennett, *J. Vac. Sci. Technol. A* **7**, 2758 (1989).

<sup>3</sup>G. S. Selwyn, *J. Vac. Sci. Technol. B* **9**, 3487 (1991).

<sup>4</sup>R. N. Carlile, S. Geha, J. F. O'Hanlon, and J. C. Stewart, *Appl. Phys. Lett.* **59**, 1167 (1991).

<sup>5</sup>H. Ikezi, *Phys. Fluids* **29**, 1764 (1986).

<sup>6</sup>*Strongly Coupled Plasma Physics*, edited by R. J. Forrest and H. E. Dewitt (Plenum, New York, 1986).

<sup>7</sup>J.-P. Hansen and I. R. McDonald, *Theory of Simple Liquids* (Academic, London, 1986).

<sup>8</sup>D. W. Schaefer and B. J. Ackerson, *Phys. Rev. Lett.* **35**, 1448 (1975).

<sup>9</sup>R. Williams, R. S. Crandall, and P. J. Wojtowicz, *Phys. Rev. Lett.* **37**, 348 (1976).

<sup>10</sup>E. C. Whipple, T. G. Northrop, and D. A. Mendis, *J. Geophys. Res.* **90**, 7405 (1985).

<sup>11</sup>F. F. Abraham, *Adv. Phys.* **35**, 1 (1986).

<sup>12</sup>The total internal energy  $NU$  is defined to be the sum of all individual particle kinetic energies and the potential energies of all particle pairs (with imaging to the replica volumes  $V'$  neighboring the basic simulation volume  $V$  as appropriate).

<sup>13</sup>M. Amini, D. Fincham, and R. W. Hockney, *J. Phys. C* **12**, 4707 (1979).

<sup>14</sup>M. Amini and R. W. Hockney, *J. Non-Cryst. Solids* **31**, 447 (1979).